Journal of Thermal Analysis and Calorimetry, Vol. 75 (2004) 101–111

SYNTHESIS OF FERRITES
Thermal analysis of some transition metal tris(maleato)ferrates(III)

B. S. Randhawa[1*], *K. J. Sweety*, *Manpreet Kaur* and *J. M. Greneche*[2]

[1]Department of Chemistry, Guru Nanak Dev University, Amritsar 143 005, (Pb), India
[2]Laboratoire de Physique de l'Etat Condensé, UMR CNRS 6087, Université du Maine,
72085 Le Mans Cedex 9, France

(Received June 16, 2003; in revised form September 23, 2003)

Abstract

Thermal analysis of some transition metal ferrimaleate precursors, $M_3[Fe(mal)_3]_2\cdot xH_2O$ (M=Mn, Co, Ni, Cu) has been studied in static air atmosphere from ambient to 600°C. Various physico-chemical techniques, i.e. TG, DTG, DTA, XRD, IR, Mössbauer spectrometry, have been employed to characterize both the intermediates and final products. After dehydration the anhydrous precursors undergo decomposition to yield an iron(II) intermediate, $M[Fe^{II}(mal)_2]$ (M=Mn, Co, Ni, Cu) in the temperature range 160–275°C. A subsequent oxidative decomposition of iron(II) species leads to the formation of α-Fe_2O_3 and MO in the successive stages. Finally a solid-state reaction occurs between the oxides above 400°C resulting in the formation of transition metal ferrites, MFe_2O_4. The ferrites have been obtained at much lower temperature and in less time than in the conventional ceramic method.

Keywords: ferrites, precursors, solid-state reactions

Introduction

Ferrite materials were widely studied because they exhibit either hard or soft magnetic properties. Indeed they found extensive applications in radio, television, microwave and satellite communications, radars, bubble devices, audio-video and magnetic recording [1]. The preparation of ferrites by the precursor method has become a fascinating subject of interest as it yields stoichiometric, pure and single phase fine particles of ferrites. Although a detailed investigation has been yet made on thermal decomposition of transition metal oxalates/ferrioxalates [2–5], a lack of similar interest on complex ferrimaleates is noticed. Another reason for undertaking such investigations is to synthesize ferrite powders at lower temperatures and shorter times than those usually observed in conventional ceramic method. Because of their complexing ability and sensitivity to oxidation states, metal ferricarboxylates have proven to be good precursor candidates, suitable for the preparation of powdered ferrites.

---

* Author for correspondence: E-mail: balwinderrandhawa@yahoo.co.in

1388–6150/2004/ $ 20.00

Akadémiai Kiadó, Budapest
Kluwer Academic Publishers, Dordrecht

Experimental section

Ferrimaleate precursors $M_3[Fe(mal)_3]_2 \cdot xH_2O$ (M=Mn, Co, Ni, Cu) were first prepared by mixing with vigorous stirring the equimolar quantities of aqueous solutions of Fe(III) maleate, maleic acid and respective transition metal carbonate in the round bottom flask. The reaction mixture was refluxed for 24 h over a water bath. The product was then isolated from the resulting solution after the addition of excess ethanol. The precipitates were finally washed with ethanol, dried in vacuum desiccator and stored in dark to avoid any chemical transformation.

Table 1 Microanalytical data of transition metal ferrimaleates $M_3[Fe(C_2H_2C_2O_4)_3]_2 \cdot xH_2O$

Complex (precursor)		C/%	H/%	Fe/%	M/%
$Mn_3[Fe(C_2H_2C_2O_4)_3]_2 \cdot 3H_2O$	obs.	28.0	1.6	10.6	15.8
	calc.	28.4	1.8	11.0	16.3
$Co_3[Fe(C_2H_2C_2O_4)_3]_2 \cdot 6H_2O$	obs.	26.1	2.1	10.1	16.0
	calc.	26.6	2.2	10.4	16.4
$Ni_3[Fe(C_2H_2C_2O_4)_3]_2 \cdot 10H_2O$	obs.	24.4	2.6	9.4	15.1
	calc.	25.0	2.8	9.7	15.4
$Cu_3[Fe(C_2H_2C_2O_4)_3]_2 \cdot 6H_2O$	obs.	25.8	2.1	10.0	17.1
	calc.	26.3	2.2	10.2	17.4

The identities of the precursors were established by chemical analysis and the results are listed in Table 1. It is concluded that the experimental content well agree with expected ones. The iron content in various complexes was determined by spectrophotometry using 1,10 phenanthroline [6]. The transition metal (Mn, Co, Ni, Cu) content was determined by a method reported elsewhere [5].

Mössbauer studies were performed using a conventional transmission spectrometer with constant acceleration drive. A $^{57}Co(Rh)$ source diffused into a Rh matrix was employed. All Mössbauer spectra were recorded at 300 K and fitted by means of quadrupolar or magnetic components with Lorentzian lines. The isomer shift values are quoted to that of metallic iron at 300 K. IR spectra of the precursors and their thermal products were recorded in the region 4000–200 cm^{-1} on a SP3-300 (Pye-Unichem. Ltd., England) spectrophotometer in KBr matrix. XRD powder patterns were recorded at USIC, UOR, Roorkee (India) using Ni filtered CuK_{α} radiation. Simultaneous non-isothermal DSC curves (TG, DTG, DTA) were recorded on Stanton Redcroft Model (STA-780) at a heating rate of 10°C min^{-1}. To identify the intermediates and final products, the precursors were also calcinated isothermally in silica crucibles in a muffle furnace at different temperatures for different time intervals. The variation in temperature was kept within ±5°C during isothermal calcination.

Results and discussion

Infrared spectra of transition metal tris(maleato)ferrates(III) show a broad band centered at about 3280 cm^{-1} due to ν(OH) of lattice water molecules and a small but distinct shoulder at about 2925 cm^{-1} due to ν(C–H) of the maleate group. The overlapped bands due to ν(C=C) and ν_{asy}(C=O) lie in the range 1630–1660 cm^{-1} while bands ranged in 1280–1420 cm^{-1} are attributed to ν_{sym}(C=O) of the coordinated maleate groups [7]. A sharp band near 870 cm^{-1} is assigned to *cis*(C–H) wagging. Bands lying in the range 500–300 cm^{-1} mark the presence of ν(Fe–O) and ν(M–O).

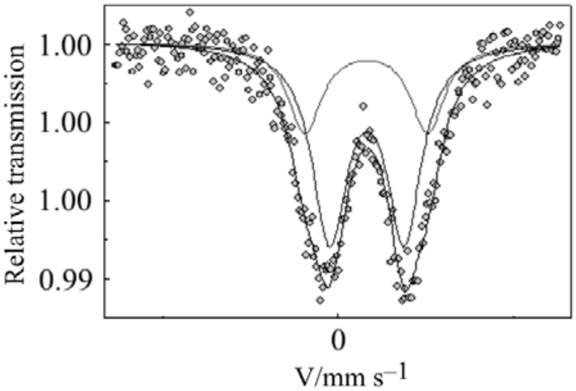

Fig. 1 Room temperature Mössbauer spectrum of copper tris(maleato)ferrate(III) hexahydrate

Mössbauer spectra of transition metal tris(maleato)ferrates(III) at 25±2°C exhibit a doublet (an example is illustrated in Fig. 1). The magnitudes of isomer shift and quadrupole splitting lie in the ranges 0.30–0.35 and 0.57–0.68 mm s^{-1} respectively. These parameters are in agreement with those reported for high spin iron(III) complexes with octahedral geometry [8]. The six coordination number of iron is satisfied by three carboxylate ligands which are bound through oxygen atoms of the maleate groups. The transition metal and water molecules seem to be responsible for linking together the complex ion [9], $[Fe(mal)_3]^{3-}$.

The decomposition behavior of each complex is discussed separately.

Manganese tris(maleato)ferrate(III) trihydrate, $Mn_3[Fe(C_2H_2C_2O_4)_3]_2\cdot 3H_2O$

Figure 2 shows the simultaneous TG, DTA and DTG curves of manganese tris(maleato)ferrate(III) trihydrate at a heating rate of 10°C min^{-1}. The slope of the TG curve shows that dehydration and decomposition of the anhydrous complex occur simultaneously until a mass loss of 16% is reached at 180°C suggesting the formation of manganese(II) and iron(II) maleates (calc. loss=16.5%). These thermal changes are accompanied by a flattened DTG peak centered at about 75°C which is endo in DTA. A further mass loss up to 22% indicates the gradual decomposition of ferrous maleate into oxalate

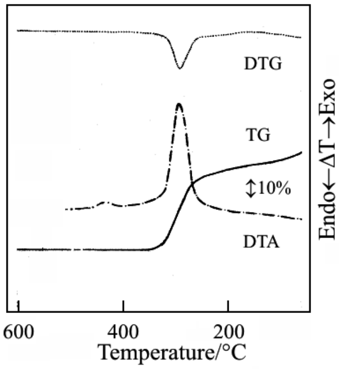

Fig. 2 Simultaneous DTG, TG and DTA curves of manganese tris(maleato)ferrate(III) trihydrate

after the elimination of acetylene (calc. loss=21.6%). There are corresponding DTG and DTA (endo) steps for this decomposition process. The identity of iron(II) species has been confirmed by Mössbauer spectrum of the residue got after calcinating the parent complex isothermally at 250°C for 15 min. The parameters of the doublet displayed in the Mössbauer spectrum (Table 3) are in close agreement to those reported for ferrous oxalate [10]. A further steep rise in mass loss up to 63.5% at 370°C suggests the oxidative

Table 2 Mössbauer parameters of the decomposition products of $M_3[Fe(C_2H_2C_2O_4)_3]_2\cdot xH_2O$ at 300 K. Isomer shift values δ are given relative to that of metallic iron at 300 K. Δ quadrupolar splitting and $2\in$ quadrupolar shift; B hyperfine field

M	Calcinating temp./°C	δ/mms^{-1}	Δ or 2ε/mms^{-1}	B/T	Fe^{3+} distribution	Assignment
Mn	250	1.21	1.78	–	–	FeC_2O_4
	370	0.35	–	50.3	–	α-Fe_2O_3
	500	0.38	–0.21	51.5	46% (oct)	$MnFe_2O_4$
		0.28	–0.29	50.2	54% (tet)	
Co	160	1.29	2.88	–	–	$Co[Fe^{II}(C_2H_2C_2O_4)_2]$
	360	0.38	–	50.9	–	α-Fe_2O_3
	500	0.37	–0.12	51.6(S)	36% (oct)	$CoFe_2O_4$
		0.28	–0.01	48.8(S)	59% (tet)	
		0.34	0.51	(CD)	5%	
Ni	400	0.37	–	51.0	–	α-Fe_2O_3
	500	0.36	–	52.0(S)	50% (oct)	$NiFe_2O_4$
		0.26	–	48.1(S)	39% (tet)	
		0.30	0.74	(CD)	11%	
Cu	300	0.35	–	51.1	–	α-Fe_2O_3
	350	0.37	–0.22	51.0	47% (oct)	$CuFe_2O_4$
		0.27	–0.03	47.8	53% (tet)	

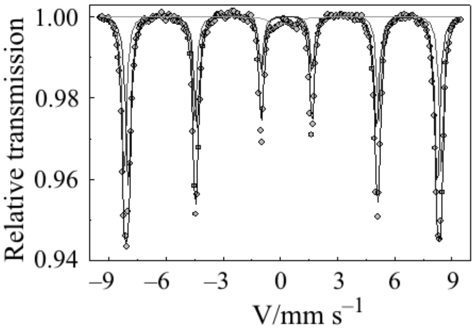

Fig. 3 Room temperature Mössbauer spectrum of the final product of manganese ferrimaleate

decomposition of these intermediate products into their respective oxides as shown by DTG and DTA (exo) peaks at 328 and 332°C respectively. The presence of α-Fe_2O_3 has been confirmed by Mössbauer spectrometry of the residue obtained by calcinating the parent complex isothermally at 370°C for 15 min. The refined Mössbauer parameters of the sextet, listed in Table 2, agree with those reported for α-Fe_2O_3 [11].

At higher temperatures a solid-state reaction occurs between manganese oxide and α-Fe_2O_3 (as supported by a small distinct exotherm at 450°C) to yield manganese ferrite, $MnFe_2O_4$. The existence of manganese ferrite has been confirmed by Mössbauer spectrometry (Fig. 3) of the final residue which displays two superimposed sextets with parameters which are consistent with those reported for $MnFe_2O_4$ [12]. Mössbauer parameters of various products are summarized in Table 2. Formation of manganese ferrite has been further confirmed by XRD powder pattern of the final residue (Table 3).

Table 3 Room temperature XRD powder data of the final product of manganese ferrimaleate

Experimental			ASTM data*		
d/Å	I_{rel}	hkl	d/Å	I_{rel}	Assignment
3.011	32	220	3.005	35	$MnFe_2O_4$^{a}
2.562	100	311	2.563	100	$MnFe_2O_4$
2.227	93	200	2.223	100	MnO^b
1.576	57	220	1.571	60	MnO
1.508	40	440	1.503	40	$MnFe_2O_4$
1.336	18	311	1.340	20	MnO
1.300	21	533	1.296	20	$MnFe_2O_4$
1.100	20	731	1.106	20	$MnFe_2O_4$

*ASTM card number a) 10-319, b) 7-230

Cobalt tris(maleato)ferrate(III) hexahydrate, $Co_3[Fe(C_2H_2C_2O_4)_3]_2\cdot 6H_2O$

Simultaneous TG, DTA and DTG curves of the precursor are displayed in Fig. 4. Dehydration does not show a stable plateau in TG but occurs along with decomposition until a mass loss of 23% is reached at 160°C with a broad DTG peak centered at 92°C which is endo in DTA. This mass loss agrees with the formation of iron(II) species and cobalt oxalate (calc. loss=22.9%). The identity of iron(II) intermediate as $Co[Fe^{II}(C_2H_2C_2O_4)_2]$ has been confirmed by Mössbauer spectrometry of the residue obtained by firing the parent complex isothermally at 160°C for 15 min. The parameters of the doublet are comparable to those reported [13] for $[Fe(ox)_2]^{2-}$. As heating continues these intermediate products undergo multistep oxidative decomposition process as shown by DTG curve and an exothermic region in DTA from 192 to 428°C. A final mass loss of 64% at 360°C corresponds to the formation of cobalt oxide and α-Fe_2O_3 which undergo a solid-state reaction at higher temperature to yield cobalt ferrite, $CoFe_2O_4$ at 428°C. The existence of cobalt ferrite has been revealed by the Mössbauer spectrum of the final product (Fig. 5) which exhibits a complex Zeeman pattern consisting of two sextets and a central doublet. The simultaneous

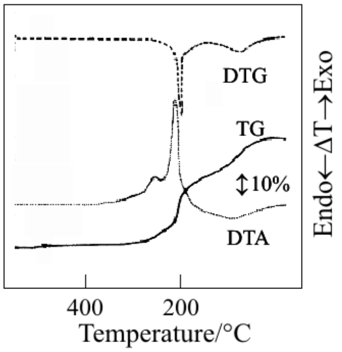

Fig. 4 Simultaneous DTG, TG and DTA curves of cobalt tris(maleato)ferrate(III) hexahydrate

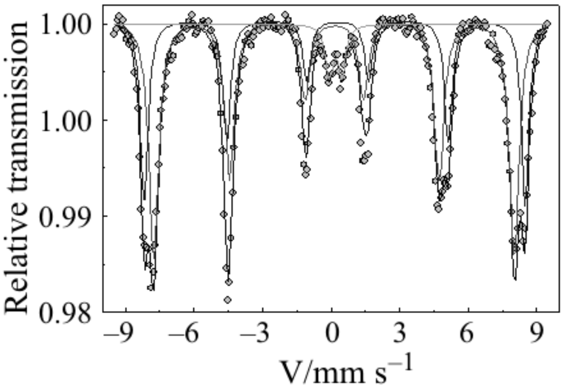

Fig. 5 Room temperature Mössbauer spectrum of the final product of cobalt ferrimaleate

presence of the two sextets and a central doublet suggest the coexistence of ferrimagnetism and superparamagnetism phenomena [14].

XRD pattern of the end product has further confirmed the presence of cobalt ferrite along with cobalt oxide (Table 4).

Table 4 Room temperature XRD powder data of the final product of cobalt ferrimaleate

Experimental			ASTM data*		
d/Å	I_{rel}	hkl	d/Å	I_{rel}	Assignment
3.00	18	220	2.97	20	$CoFe_2O_4$^{a}
2.50	100	311	2.53	100	$CoFe_2O_4$
2.41	72	111	2.46	75	CoO^b
2.15	95	200	2.13	100	CoO
2.05	19	400	2.08	20	$CoFe_2O_4$
1.65	36	333	1.61	40	$CoFe_2O_4$
1.47	65	440	1.48	64	$CoFe_2O_4$
1.30	20	311	1.28	20	CoO

*ASTM Card number a) 3-0864, b) 9-402

Nickel tris(maleato)ferrate(III)decahydrate $Ni_3[Fe(C_2H_2C_2O_4)_3]_2\cdot 10H_2O$

Figure 6 shows the simultaneous TG, DTA and DTG curves of nickel tris(maleato)ferrate(III) decahydrate at a heating rate of 10°C min^{-1}. TG does not show any stable plateau for dehydration and decomposition up to 300°C. However DTG shows three steps with peak temperatures of 66, 107, 192°C respectively which are endo in DTA. The first two endotherms correspond to the elimination of water molecules in two consecutive batches of four and six with mass losses of 6.5 and 16% respectively (calc. loss=6.2 and 15.6%, respectively). The third endotherm is associated with the formation of iron(II) intermediate i.e. $Ni[Fe(C_2H_2C_2O_4)_2]$ and nickel oxalate as indicated by a mass loss of 28% at

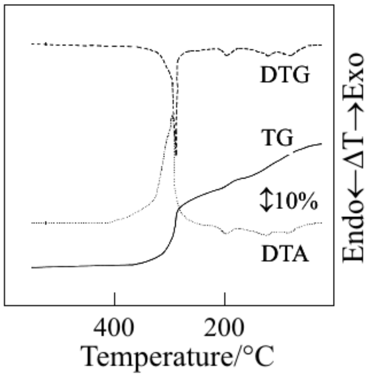

Fig. 6 Simultaneous DTG, TG and DTA curves of nickel tris(maleato)ferrate(III) hexahydrate

275°C (calc. loss=28.1%). Since iron(II) species did not give a stable plateau, hence could not be detected by Mössbauer spectrometry. A further abrupt mass loss up to 66.5% suggests the oxidative decomposition of the intermediate products into their respective oxides at 399°C (calc. loss=66.6%). This thermal process is accompanied by a strong DTG peak at 310°C (along with a shoulder) and an exothermic region from 275 to 460°C. The existence of iron(III) oxide as α-Fe_2O_3 has been confirmed by the Mössbauer parameters of the residue (Table 2). Beyond 400°C, a solid-state reaction is supposed to take place between nickel oxide and α-Fe_2O_3 to give nickel ferrite, $NiFe_2O_4$. Formation of nickel ferrite as the end product has been confirmed by Mössbauer spectrum and XRD powder pattern (Table 5) of the final residue. The shape and parameters of Mössbauer spectrum are almost similar to the ones obtained from the heat treated nickel ferrioxalate [4].

Table 5 Room temperature XRD powder data of the final residue of nickel ferrimaleate

Experimental			ASTM data*		
d/Å	I_{rel}	*hkl*	*d*/Å	I_{rel}	Assignment
2.940	27	220	2.948	30	$NiFe_2O_4$[a]
2.510	100	311	2.513	100	$NiFe_2O_4$
2.400	85	222	2.410	90	NiO[b]
2.080	24	400	2.085	25	$NiFe_2O_4$, NiO
1.600	28	511	1.605	30	$NiFe_2O_4$
1.475	40	440	1.476	40	$NiFe_2O_4$, NiO
1.090	15	731	1.086	16	$NiFe_2O_4$
0.930	20	840	0.932	21	$NiFe_2O_4$, NiO

*ASTM Card number a) 10-325, b) 4-0835

Copper tris(maleato)ferrate(III) hexahydrate, $Cu_3[Fe(C_2H_2C_2O_4)_3]_2 \cdot 6H_2O$

The simultaneous TG, DTA and DTG curves of copper tris(maleato)ferrate(III) hexahydrate are displayed in Fig. 7. Dehydration occurs in two steps as shown by the corresponding DTG

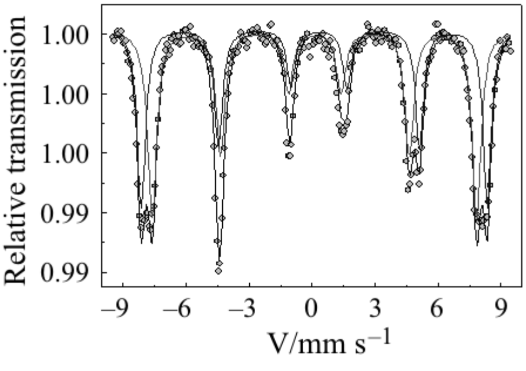

Fig. 7 Simultaneous DTG, TG and DTA curves of copper tris(maleato)ferrate(III) hexahydrate

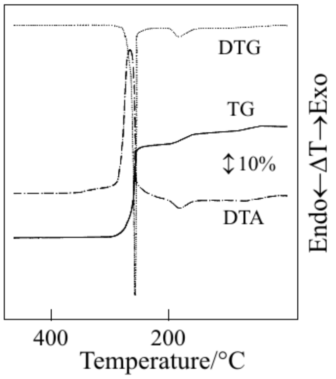

Fig. 8 Room temperature Mössbauer spectrum of the final product of copper ferrimaleate

peaks at 65 and 160°C which are endo in DTA. In first installment, there is an elimination of two water molecules followed by the removal of another batch of the remaining four with respective mass losses of 3.0 and 10% up to 185°C. The anhydrous complex, after remaining stable up to 215°C, undergoes an abrupt change in mass loss up to 64% accompanied by intense DTG and DTA (exo) peaks at 255 and 261°C respectively. This oxidative decomposition step is associated with a mass loss of 63.5% suggesting the formation of copper oxide and α-Fe_2O_3 (calc. loss=63.6%). As heating continues, a solid state reaction occurs between the oxides above 300°C to yield copper ferrite, $CuFe_2O_4$. The existence of ferrimagnetic copper ferrite has been confirmed by Mössbauer spectrometry (Fig. 8) of the end product which exhibits two sextets with parameters cited in Table 2. These parameters are in agreement with those reported [15] for $CuFe_2O_4$. Formation of copper ferrite has been reaffirmed by XRD powder pattern of the final residue (Table 6).

Table 6 Room temperature XRD powder data of the final residue of copper ferrimaleate

Experimental			ASTM data*		
d/Å	I_{rel}	hkl	d/Å	I_{rel}	Assignment
4.75	28	111	4.79	30	$CuFe_2O_4$[a]
2.99	51	220	2.96	50	$CuFe_2O_4$
2.51	100	311	2.52	100	$CuFe_2O_4$, CuO
2.30	90	111	2.32	96	CuO[b]
2.12	32	400	2.10	30	$CuFe_2O_4$
1.84	24	202	1.87	25	CuO
1.60	36	511	1.61	40	$CuFe_2O_4$
1.45	55	440	1.48	60	$CuFe_2O_4$
1.36	20	220	1.38	19	CuO
1.25	18	533	1.27	20	$CuFe_2O_4$
1.09	27	731	1.087	30	$CuFe_2O_4$

*ASTM Card number a) 25-283, b) 5-0661

On the basis of various thermoanalytical techniques employed during the aerial pyrolysis of transition metal tris(maleato)ferrates(III) it is proposed that the thermal reaction occurs in three main consecutive steps:

i) Dehydration of the precursor

ii) Reduction of the anhydrous complex to iron(II) state

iii) Reoxidation of the iron(II) moiety to α-Fe_2O_3 followed by its solid-state reaction with a transition metal oxide to yield ferrite.

Magnetic properties of transition metal ferrites

The transition metal ferrites are magnetic materials which find an extensive application in home appliances, electronic products, automobiles, communication equipments and data processing devices. These materials have now become a vital part of everyday life in modern electronic industry. The intrinsic magnetic properties such as saturation magnetization, Curie temperature etc. possessed by the ferrites make them suitable to operate at microwave frequencies where pure metals are less applicable. Various magnetic properties of the ferrites obtained are listed in Table 7. All the materials show Curie temperatures in close agreement with the reported values [1]. It has been observed that the ferrites obtained from the thermal reactions of ferrimaleate precursors (Table 7) show higher magnitudes of saturation magnetization than the ones got from respective ferrioxalates [3], thus making the former more suitable/potential materials to operate at high frequencies [16]. A detailed explanation of magnetic properties would require the estimation of metal transition contents in both tetrahedral and octahedral units. The present values differ a priori from those observed in ferrites prepared by conventional methods but the accurate proportions can be achieved by ^{57}Fe in-field Mössbauer experiments which provides Fe contents in the two sites.

Table 7 Magnetic parameters of the ferrites obtained from heat treated of $M_3[Fe(mal)_3]_2 \cdot xH_2O$. Density and Curie temperatures are compared to those observed on ferrites prepared by conventional methods (values given in parenthesis)

MFe_2O_4	Density/g cm^{-3}	Specific magnetization/ Gauss/cm^3	Saturation magnetization/ Gauss	T_c/K
$MnFe_2O_4$	3.13 (5.00)	805	2520	588 (573)
$CoFe_2O_4$	4.16 (5.29)	765	3182	791 (793)
$NiFe_2O_4$	3.52 (5.38)	700	2464	856 (858)
$CuFe_2O_4$	3.96 (5.42)	705	2792	721 (728)

Conclusions

Microcrystalline ferrites have been obtained from the thermal reactions of the transition metal ferrimaleates at a temperature (350–500°C) much lower than that of alkali/alkaline earth ferrimaleates [17, 18] (450–600°C). This is due to the direct decomposition of the former into oxide phase. These temperatures of ferrite formation are also quite lower than for the ceramic method [19, 20]. Another attractive feature of the method used is that it does not involve milling stages of the precursor which is necessary in the ceramic method. The milling introduces defects and strains in the ferrite obtained which in turn affect its permanent magnetic properties, which are strongly dependent on the microstructure.

References

1 B. Viswanathan and V. R. K. Murthy, Ferrite Materials, Springer-Verlag, Berlin, 1990.
2 B. Malecka, E-D. Ciesla, A. Malecki, J. Therm. Anal., 68 (2002) 819.
3 O. Carp, L. Patron, G. Marinescu, G. Pascu, P. Budrugeac, M. Brezeanu, J. Therm. Anal., 72 (2003) 263.
4 D. Dollimore and D. L. Griffiths, J. Thermal Anal., 2 (1970) 229.
5 B. S. Randhawa, J. Mater. Chem., 10 (2000) 2847.
6 A. I. Vogel, A Text Book of Quantitative Inorganic Analysis including Elementary Instrumental Analysis, Eng. Lang. Book Soc. and Longman, London 1973, p. 786.
7 K. Nakamoto, Infrared Spectra of Inorganic and Coordination Compounds, John Wiley Intersci., New York 1970.
8 A. Vertes, L. Korecz and K. Burger, Mössbauer Spectroscopy, Elsevier, New York 1979, p. 47.
9 A. S. Brar and B. S. Randhawa, J. Phys., 44 (1983) 1385.
10 M. J. Halsey and A. M. Pritchard, J. Chem. Soc.(A), (1968) 2878.
11 D. E. Cox, G. Shirane and S. L. Ruby, Phys. Rev., 125 (1962) 1163.
12 A. H. Morrish, Z. W. Li and X. Z. Zhou, J. Phys. IV, 7 (1997) C1-513.
13 H. Sato and T. Tominaga, Bull. Chem. Soc. Japan, 55 (1979) 1402.
14 O. G. Mandada, K. B. Modi, K. M. Jadhav and G. K. Bichile, Indian J. Pure and Appl. Phys., 35 (1997) 554.
15 B. J. Evans and S. S. Hafner, J. Phys. Chem. Solids, 29 (1968) 1573.
16 Kirk-Othmer, Encyclopedia of Chemical Technology, 3rd Ed., Vol. 14, Wiley Intersci. Publ., USA, 1981.
17 B. S. Randhawa and K. J. Sweety, J. Therm. Anal. Cal., 62 (2000) 275.
18 B. S. Randhawa and K. J. Sweety, J. Radioanal. Nucl. Chem., 247 (2001) 513.
19 M. J. Ruthner, J. Phys. IV, 7 (1997) C1-53.
20 G. M. Jeong and S. S. Kim, J. Mag. Soc. Japan, 22 (1998).